

Declaration of Authorship Correction: Addition of Missing Author

Journal: International Journal of Integrated Engineering

Article Title: Characterization of Biomaterials with Rose Petal Properties by Adapting Hyperelastic Models

Volume: Vol. 16 No. 8

DOI: <https://doi.org/10.30880/ijie.2024.16.08.022>

Upon notification and agreement from all co-authors, it has been brought to our attention that one author was unintentionally omitted from the original publication. The following author has now been officially added to the author list:

Added Author

Name: Nur Shahira binti Mohd Arif

Affiliation: School of Mechanical Engineering, College of Engineering, Universiti Teknologi MARA, 40450 Shah Alam, Selangor, MALAYSIA

Email: shahira.arif75@gmail.com

Contribution: Contributed to execution of experiments and data collection.

This correction has been made with the consent of all authors and verified by the editorial office. The amendment does not affect the scientific integrity, results, or conclusions of the published article.

This cover note serves as an official declaration. It is attached to the article for transparency and to maintain the accuracy and integrity of the publication.

If you have any questions or concerns regarding this matter, please contact the journal's editorial office.

Sincerely,

Editorial Board of International Journal of Integrated Engineering (IJIE)

Characterization of Biomaterials with Rose Petal Properties by Adapting Hyperelastic Models

Muhammad Iman Sufi Suliman¹, Nur Shahira Mohd Arif¹, Abdul Malek Abdul Wahab¹, Muhammad Ilham Khalit², Abdul Halim Abdullah¹, Nor Fazli Adull Manan^{1*}

¹ School of Mechanical Engineering, College of Engineering,
Universiti Teknologi MARA, 40450 Shah Alam, Selangor, MALAYSIA

² Department of Mechanical Engineering, School of Engineering,
Bahrain Polytechnic, 5G7V+7GP, Isa Town, BAHRAIN

*Corresponding Author: norfazli@uitm.edu.my

DOI: <https://doi.org/10.30880/ijie.2024.16.08.022>

Article Info

Received: 3 July 2024

Accepted: 24 October 2024

Available online: 30 December 2024

Keywords

Skin substitute, silicone rubber, rose petal, tensile test, hyperelastic models

Abstract

The rose petals will be used together with other biomaterial compositions that would fit in artificial skin composition-based to improve the enhancement of healing agents. The objective of this project is to develop biomaterial with the enhancement of rose petals which acts as a healing agent for skin substitutes, and to characterize its mechanical properties that suit hyperelastic models. The methodology process involves mixing silicone rubber, gelatin, glycerin, distilled water, and rose petal powder to carry out the mechanical properties and hyperelastic behavior that could mimic the skin of mechanical properties. A double-boiling process was used and continuously stirred the mixtures up to 90°C before being poured into the 3D print mold. ASTM D412 is a uniaxial tensile test standard with a constant speed rate of 50 mm/min that was used in this study. The raw data from the computational Load-Extension was plotted on a graph of stress-strain and stress-stretch. The numerical approach of hyperelastic models such as Mooney-Rivlin and Yeoh are selected to analyze stress-stretch of biocomposite of skin substitute. The constant, C_1 , is in the range of 0.0344-0.0385 MPa, while C_2 is in the negative range of 0.0365-0.0829 MPa, according to the Mooney-Rivlin model results. Meanwhile, for the Yeoh model, the constant, C_p , is in the range of 0.00695-0.0122 MPa. The combination of silicone rubber, gelatin, glycerin, distilled water, and rose petal powder is homogeneous because lies within the skin's mechanical properties range. This study has significantly contributed to a better understanding of the mechanical properties of biocomposite.

1. Introduction

A biomaterial may be defined as a material used in the production of prostheses and biomedical devices that are meant to replace or restore the function of a body that is affected according to da Silva et al. [1]. Bharadwaj said that biomaterials are used in various parts of the human body, such as shoulders and knee replacement implants, hips, elbows, ears, and orthodontics [2]. The absence of decent constitutive skin models is partly owing to the difficulty of quantifying skin's mechanical properties. As a result, researchers often use animal skin instead of human tissue in understanding human skin. According to Freedman and Mooney, mechanical testing on animal

This is an open access article under the CC BY-NC-SA 4.0 license.



skin benefits from abundant tissue, gene mutations, and the capability of manipulating tissue conditions to induce tissue scarring or stimulate hormone changes [3]. In fact, murine and human skin share the same anatomical and biomechanical characteristics as both have three primary layers and are anisotropic, which are nonlinear, heterogeneous, and viscoelastic properties that can be affected by donor age and hydration refer to Wahlsten et al. [4]. A computer model with mechanical qualities like human skin would be ideal for replacing, reducing, or refining the usage of animal models in industries such as dermatology, wound healing, medical device development, and the cosmetic industries. Besides, with the help of imaging techniques such as motion analysis and digital image correlation, the strain distribution in the skin has been mapped out by Chen, Genovese, and Pan [5]. However, measurements of tensile strength done on skin samples that have been removed allow for greater strains to be applied at different points on different paths, which gives useful anisotropic data about large levels of deformation.

Moreover, Mostafavi Yazdi & Baghersad [6] said that many nonlinear isotropic constitutive models have been employed to characterize skin mechanical properties, such as the Ogden, Mooney Rivlin, and Neo-Hookean. Additionally, Tang, Richardson & Anseth [7] mention that various other soft tissues contain a fibrous matrix that contributes to their mechanical properties. As a result, various constitutive models using a fibrous network have been constructed. Some of them have also been used to model ligaments, blood arteries, heart tissue, and skin. Once the results are obtained, a model is needed to fit the results. According to Ansarri-Benam & Bucchi [8], the phenomenological approach proposes strain energy functions that attempt to match the data in a mathematical way. As a result, the material parameters present in these models usually have no physical significance. The procedure is fast and easy, but it loses touch with reality and physical sense. Other approaches by Dai, Shih, & Khachemoune [9], consequently, try to model the inner structure to some extent and give material parameters certain physical significance. The problem is that it's usually difficult to get a model that works well.

Furthermore, only one type of experimental test is generally applicable, namely, a uniaxial tension test. Thus, this study aims to use biomaterial as the composition for the artificial skin, whereas the chosen base material is silicon rubber. Silicone rubber is widely used in the medical field for such things as aesthetic implants, and medical disposable supplies. Moreover, it is also used in synthetic skin substitutes like Biobrane, Integra, and TransCyte by Ahmed et al. [10]. Meanwhile, gelatin is known for having the same physical properties of density, stiffness, energy dissipation, and ballistic performance as human skin. However, it has limited usage as it is poor in shape, poor in mechanical properties, and has less elasticity and thermal stability according to Lee et al. [11]. The other materials utilized in this experiment are distilled water and glycerin, with the enhancement of rose petal extract as a skin anti-inflammatory refer to Scaffaro, Maio, & Citarrella [12]. This rose petal extract is used as a healing agent to treat a variety of ailments, including wounds, inflammation, sunburns, and many others. Hence, rose petals will be used together with other biomaterial compositions that would fit into an artificial skin composition-based to improve the enhancement of healing agents and to characterize their mechanical properties that suit hyperelastic models since different materials have developed different strengths.

Rose petals are great for hair, especially when mixed with other restorative ingredients like oil, honey, and rosemary oil. It gives the skin significant hydration and nourishment while also giving the hair power and strength by Saini et al. [13]. The rose petal also had been tested on the pH test viscosity to avoid any skin irritation. Therefore, Heo et al. [14] would also synthesize a new material composition that could mimic skin mechanical properties with the future potential to replace or encourage physiological functions of a component of the human body. This clearly highlights the needs of rose petal as a new agent for the enhancement of healing agent.

2. Methodology

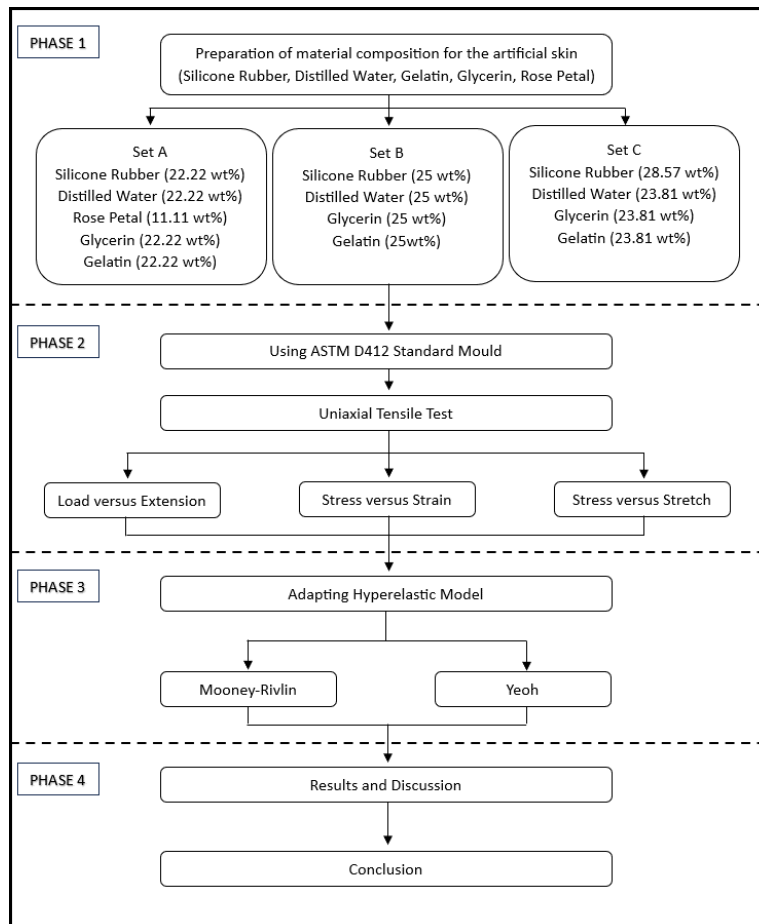
2.1 Sample Preparation

The main material used in the composition of artificial skin is silicon rubber, with additional materials of gelatin, glycerin, distilled water, and rose petal extract. The rose petal extract contains the nutritional breakdown of the powdered dried rose petals as follows: 84.5% moisture, 0.4g ash, 70.4g carbohydrate, 0.5 g protein, 0.2g fat, 1.2g crude fiber, 0.2mg vitamin C, 3.7mg iron, and 120mg calcium [15]. The sample preparation is conducted in the Advanced Material Laboratory, School of Mechanical Engineering, College of Engineering, UiTM Shah Alam. Basically, the materials are weighed by using an analytical balance before being mixed in a 50 ml beaker according to their weight percent and stirred with a spatula. The mixtures then undergo a double boiling process and are continuously stirred at a constant heating temperature of 90°C before being poured into the 3D-printed mold. After that, the sample is stored in a refrigerator at 7°C for 24 hours to enhance its strength. As shown in Fig. 1, the same steps are repeated for each material composition.

Table 1 shows the comparison between each set. Set A and Set B were compared in terms of the presence of the rose petal. As mentioned before, the rose petal will bring improvement in terms of healing agents. On the other hand, Set A and Set C were compared in terms of the composition of the silicone rubber. As their own characteristic, silicone rubber can improve the elasticity to the artificial skin.

Table 1 The specific weight of the material composition for each set of artificial skin

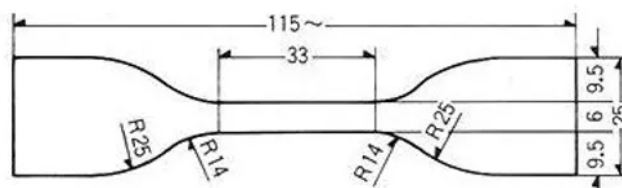
	Silicone Rubber (g)	Distilled Water (g)	Gelatin (g)	Glycerin (g)	Rose Petal Extract (g)
Set A	12.5	12.5	12.5	12.5	12.5
Set B	12.5	12.5	12.5	12.5	0
Set C	15.0	12.5	12.5	12.5	0

**Fig. 1** The flowchart involved in this study

2.2 Mold Preparation

The standard ASTM D412 mold is sketched in CATIA V5R21 according to the schematic diagram in Fig. 2 and Fig. 3 to visualize the actual dimensions of the sample.

After that, the STL file (.stl) is imported into Ultimaker Cura to generate its G-code before 3D print by using Ender 3 Max printer. The printing hour took approximately 11 hours and 4 minutes as shown in Fig. 4. A total of 5 samples are prepared for each set of composition material.

**Fig. 1** The schematic drawing of standard ASTM D412 in mm unit

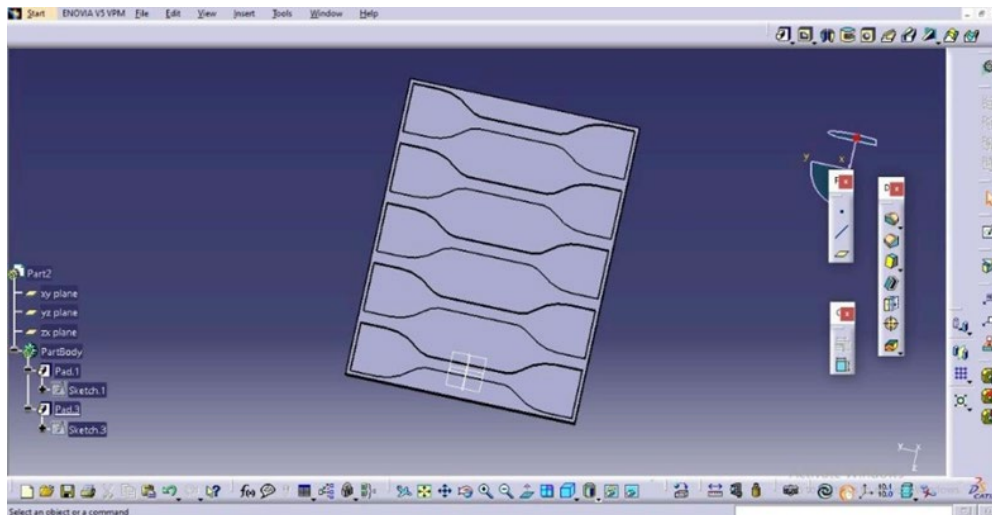


Fig. 2 The CATIA drawing of standard ASTM D412 mold

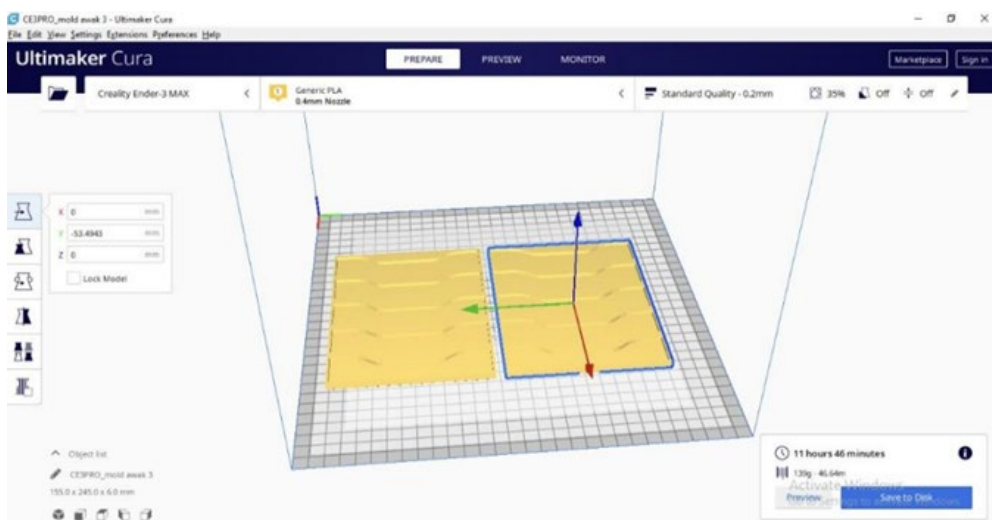


Fig. 3 The setting up of the 3D print mold in Ultimaker Cura

2.3 Experimental Procedures

The uniaxial tensile test has been conducted using Universal Testing Machine (SHIMADZU AG-IC) in the Concrete Laboratory, School of Civil Engineering, College of Engineering, UiTM Shah Alam. The sample is mounted to the jig of the tensile machine by clamping the sample to the jig at a constant speed rate of 50 mm/min. Then, the sample was tested until it ruptured into two parts. Before removing the sample from the jig, be sure the machine had totally stopped. The same method was used for all sets.

2.4 Data Extraction

The raw data obtained from the computer is generated in the spreadsheet files which contain results of time, load, and extensions. Hence, the graph of load-extension, stress-strain, and stress-stretch is plotted. The numerical approach of hyperelastic models such as Mooney-Rivlin and Yeoh is applied to analyze stress-stretch of biocomposite of artificial skin.

3. Result and Discussion

The raw data of the experiment is used to obtain the graph of load-extension, stress-strain, and stress-stretch. The experimental result obtained is also significant for the numerical method since it will be utilized to calculate the material constants using the Mooney Rivlin and Yeoh model. The physical condition of the sets after undergoing the tensile test is shown in Fig. 5.

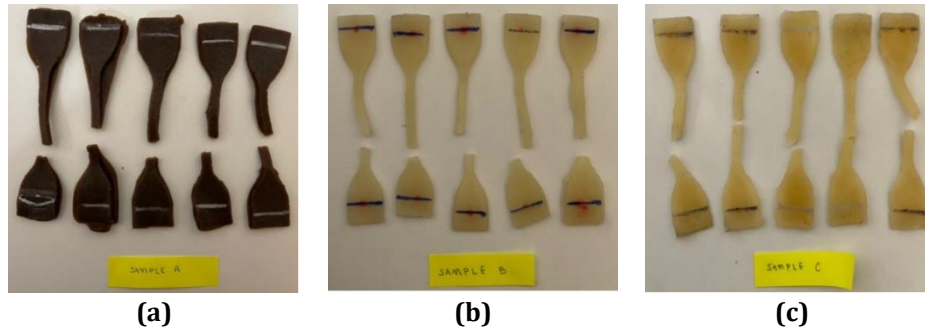


Fig. 4 (a) Set A; (b) Set B; (c) Set C

3.1 Load Versus Extension

Load and extension data from uniaxial tensile tests were converted into a Load-Extension graph to facilitate data analysis. The tensile stress range of the data chosen to plot the graph altered the trend of the Load-Extension curve.

Based on Fig. 6, the extension rate for all sets increases steadily with the applied load. The elongation trend for Set C is more elongated within the range of 10.938 N until 12.500 N compared to Set A which slightly elongated within the range of 9.375 N until 10.938 N.

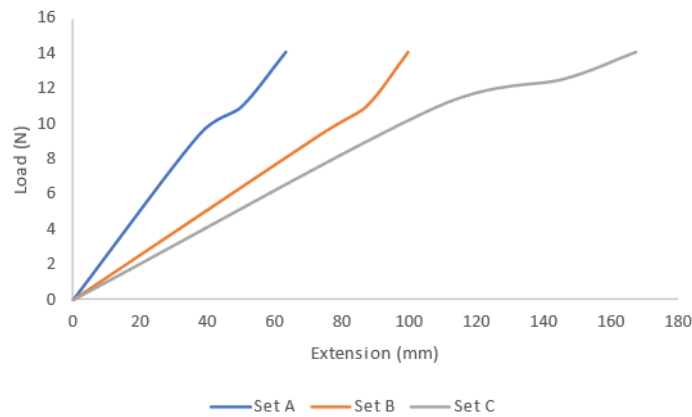


Fig. 5 The graph of load versus extension

3.2 Stress Versus Strain

According to the Theory of Stress-Strain Energy, most incompressible materials, like biomaterials, don't have a linear curve. Because incompressible materials contain viscoelasticity, they can withstand tremendous stress.

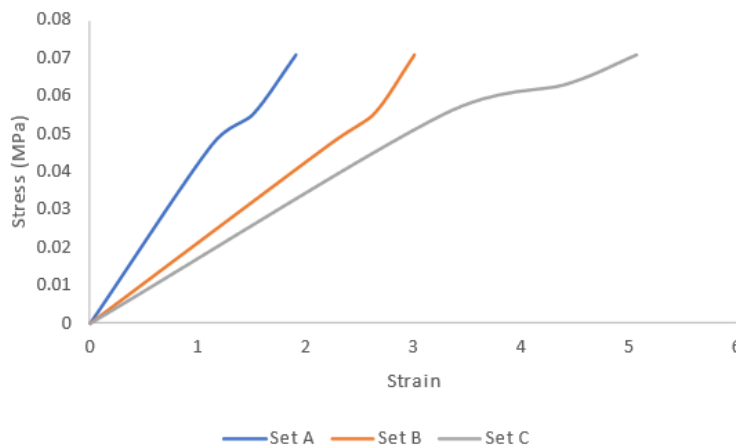


Fig. 6 The graph of stress versus strain

The trend of the curve in Fig. 7 demonstrates that Set C has the largest strain value, which is 5.078, with the highest stress level, which is 0.0710 MPa. This feature highlights Set C's noticeable flexibility, which can be largely

ascribed to Set C's higher silicone rubber composition than Set A. This elasticity comparison is important because the artificial skin that has been constructed mimics the essential qualities of human skin, which include incompressibility and high elasticity.

3.3 Standard Deviation and Variance for Stress, Strain, and Young's Modulus

To determine the mechanical properties of the material parameter, the best fit from the graph with the experimental data is critical. The more strain it is subjected to, the more elastic it becomes. To determine the small results of dispersion value, the standard deviation for tensile stress, strain, and Young's Modulus are determined. Table 2 shows the standard deviation and variance for stress, strain, and Young's modulus. It shows that Set C had higher in terms of stress-strain due to the high composition of silicone rubber. As mentioned before, the comparison between Set A and C to see the elasticity of the samples. Based on an analysis by Ni Annaidh [16], the human skin can reach 21.6 MPa for the tensile stress in Nazali [17], the author added the gelatine-BSA into the samples. As we know, the characteristic is flexible and elastic to increase the durability of the artificial skin. So, gelatine can enhance in terms of stress and strain to close the characteristics of the human skin. As compared to Nazali's data, when the silicone rubber mixed with gelatine -BSA produced 1.468 MPa.

Table 2 Standard deviation and variance values for stress, strain, and Young's modulus

	Set A	Set B	Set C
Tensile Stress (MPa)	0.0579	0.0579	0.0631
Standard Deviation	0.0121	0.0121	0.00789
Variance	0.000145	0.000145	6.22E-5
Tensile Strain	1.522	2.626	4.254
Standard Deviation	0.391	0.395	0.910
Variance	0.153	0.156	0.829
Young's modulus (MPa)	0.0384	0.0219	0.0151
Standard Deviation	0.00286	0.00141	0.00157
Variance	8.165	1.986	2.466

3.4 Biomechanical Properties

The biomechanical parameters employed for data analysis are sample stress and stretch. The materials utilized are Mooney-Rivlin and Yeoh hyperelastic. These models would contribute to predicting the biomechanical properties of samples such as artificial and biological human skins. Human skin has hyperelasticity characteristics that allow it to withstand a wide range of stresses and strains [18]. Thus, hyperelastic material constants are required to understand the biomechanical behavior of material compositions. Nazali's data had shown when the stress reached 0.8 MPa, the stretch of the sample was 4.635 [17].

Fig. 8 shows the trend of the stress-stretch curve, whereas Set C has the maximum value of stretch ratio at 6.078 meanwhile Set A has the lower value of stretch ratio to be compared despite having the same maximum stress. The composition of silicone rubber affects the stress-stretch as shown in Fig. 8. The higher the composition the more elastic the samples.

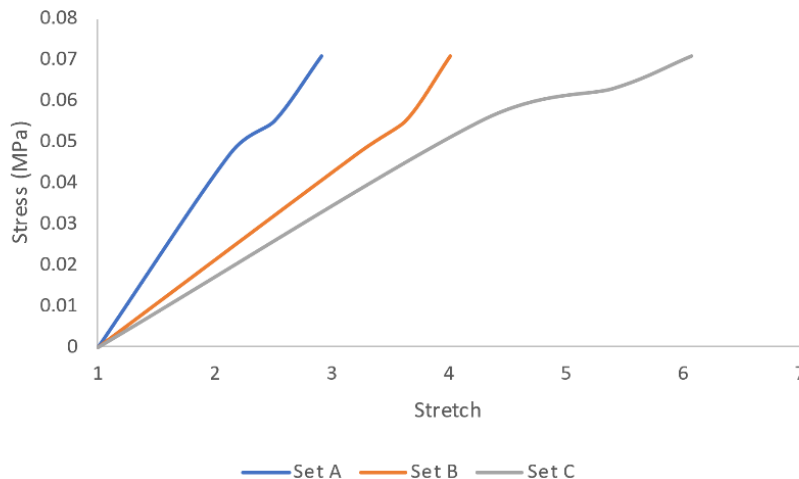


Fig. 7 The graph of stress versus stretch

3.5 Numerical Comparison

The hyperelastic of the Mooney-Rivlin and Yeoh models were used to compare the material composition. Both models are more suitable for elastomer samples. Table 3 explains the constant value for the Mooney-Rivlin and Yeoh models. The values of the parameter C_2 are negative, however, the condition of a Mooney-Rivlin material in which one of the model coefficients can be negative, but the shear modulus is always positive under small strain [19].

Table 3 The comparison between Mooney-Rivlin and Yeoh model values

Hyperelastic Model	Parameters (MPa)	Set A	Set B	Set C
Mooney Rivlin	C_1	0.0138	0.0147	0.0042
	C_2	-0.0039	-0.0239	0.0098
Yeoh	C_P	0.0046	0.0022	0.0011

The result shows the parameters of Mooney Rivlin's model and Yeoh's model after the experimental value. The experimental value will be compared to the numerical approach as the lines of the curve represent the experimental, Mooney-Rivlin, and Yeoh curves respectively. Fig. 9 to Fig. 11 was observed to compare the stress-stretch graphs of experimental and numerical approaches. Significantly, all sets show the curve trend which is increasing but different patterns from each other. As can be seen, both Model is the closest to the experimental curves, but they have a different pattern of curves. As referred to in the previous research by Adull Manan [20] about bovine skin undergoing the uniaxial tensile test, Ogden has close data to the experimental value. The result can be considered as not having close agreement with the experimental result. This is due to the average value of material constants obtained for each of the models.

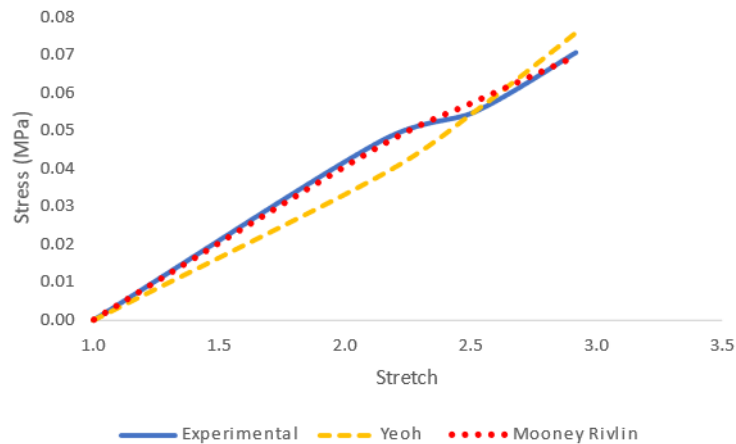


Fig. 8 The comparison between models for sample A

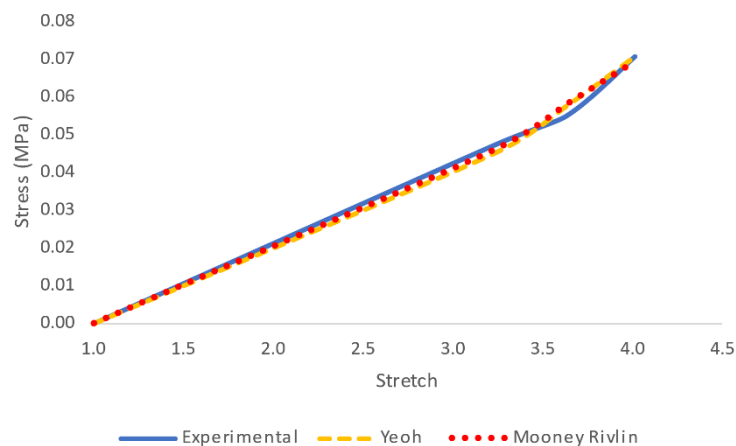


Fig. 9 The comparison between models for sample B

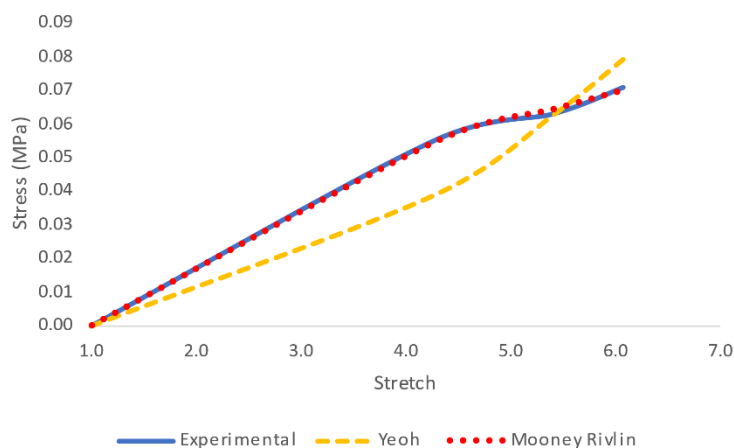


Fig. 10 The comparison between models for sample C

4. Conclusion

The optimum sample for the artificial skin in terms of biomechanics is Set B because the experimental data was closer to the hyperelastic model which is Mooney-Rivlin and Yeoh. Even though Set C had higher in terms of tensile stress, strain, and Young's Modulus. The rose petal extract might not be effective in terms of elasticity, but it will affect more on the healing agent. So, this investigation should be continued with different biomaterial compositions and another hyperelastic model such as the Ogden model. This would allow for novel material compositions with better mechanical and biomechanical capabilities. Further research will uncover a new novel skin substitute that will benefit the injured not only in terms of healing but also in terms of cost. Further research might also enhance the correlation between mechanical and biomechanical properties in developing new skin mimics that work like temporary skin substitutes yet act like permanent skin substitutes, such as a wound patch. This will help injured individuals save money on applications and speed up their recovery. May the findings of this investigation benefit society.

Acknowledgement

The authors wish to extend our sincere gratitude to the Ministry of Higher Education, the College of Engineering at UiTM Shah Alam, and all of the members of the team for providing us with the resources and assistance that we needed in conducting this research. We are incredibly grateful to everyone who helped out with this project by giving their time, expertise, and support. Your combined contributions have greatly improved the final product of this article. This research received no specific grant from any funding agency in the public, commercial, or not-for-profit sectors.

Conflict of Interest

Authors declare that there is no conflict of interest regarding the publication of the paper.

Author Contribution

The authors confirm contribution to the paper as follows: **study conception and design:** Muhammad Iman Sufi, Nor Fazli Adull Manan; **data collection:** Nur Shahira Mohd Arif, Muhamad Iman Sufi Suliman; **analysis and interpretation of results:** Muhammad Iman Sufi Suliman, Abdul Malek Abdul Wahab, Muhammad Ilham Khalit; **draft manuscript preparation:** Muhammad Iman Sufi Suliman and all authors. All authors reviewed the results and approved the final version of the manuscript.

References

- [1] Silva, L. R. R. D., Sales, W.F., Compos, F. D. A. D., Sousa, J. A. G. D., Davis, R., Singh, A., Coelho, R. T. & Borgohain, B. (2021). A comprehensive review on additive manufacturing of medical devices. *Progress in Additive Manufacturing*, 6, 517–553. <https://doi.org/10.1007/s40964-021-00188-0>
- [2] Bharadwaj, A. (2021). An Overview on Biomaterials and Its Applications in Medical Science. *IOP Conference Series: Materials Science and Engineering*, 1116, 012178. <https://doi.org/10.1088/1757-899X/1116/1/012178>
- [3] Freedman, B. R. & Mooney, D. J. (2019). Biomaterials to Mimic and Heal Connective Tissues. *Advanced Materials*, 31, 1806695. <https://doi.org/10.1002/adma.201806695>

- [4] Wahlsten, A., Pensalfini, M., Stracuzzi, A., Restivo, G., Hopf, R. & Mazza, E. (2019). On the compressibility and poroelasticity of human and murine skin. *Biomechanics and Modeling in Mechanobiology*, 18, 1079–1093. <https://doi.org/10.1007/s10237-019-01129-1>
- [5] Chen, B., Genovese, K. & Pan B. (2020). In vivo panoramic human skin shape and deformation measurement using mirror-assisted multi-view digital image correlation. *Journal of the Mechanical Behavior of Biomedical Materials*, 110, 103936. <https://doi.org/10.1016/j.jmbbm.2020.103936>
- [6] Mostafavi Yazdi, S. J. & Baqersad, J. (2022). Mechanical modeling and characterization of human skin: A review. *Journal of Biomechanics*, 130, 110864. <https://doi.org/10.1016/j.jbiomech.2021.110864>
- [7] Tang, S., Richardson, B. M. & Anseth, K. S. (2021). Dynamic covalent hydrogels as biomaterials to mimic the viscoelasticity of soft tissues. *Progress in Materials Science*, 120, 100738. <https://doi.org/10.1016/j.pmatsci.2020.100738>
- [8] Anssari-Benam, A. & Bucchini, A. (2021). A generalised Neo-Hookean strain energy function for application to the finite deformation of elastomers. *International Journal of Non-Linear Mechanics*, 128, 103626. <https://doi.org/10.1016/j.ijnonlinmec.2020.103626>
- [9] Dai, C., Shih, S. & Khachemoune, A. (2020). Skin substitutes for acute and chronic wound healing: an updated review. *Journal of Dermatological Treatment*, 31, 639–648. <https://doi.org/10.1080/09546634.2018.1530443>
- [10] Ahmed, M. A., Al-Kahtani, H. A., Jaswir, I., AbuTarboush H. & Ismail E. A. (2020). Extraction and characterization of gelatin from camel skin (potential halal gelatin) and production of gelatin nanoparticles, *Saudi Journal of Biological Sciences*, 27, 1596–1601. <https://doi.org/10.1016/j.sjbs.2020.03.022>
- [11] Lee, M., Nam, T.G., Lee, I., Shin, E.J., Han, A., Lee, P., Lee, S.Y. & Lim, T.G. (2018). Skin anti-inflammatory activity of rose petal extract (*Rosa gallica*) through reduction of MAPK signaling pathway. *Food Science & Nutrition*, 6, 2560–2567. <https://doi.org/10.1002/fsn3.870>
- [12] Scaffaro, R., Maio A. & Citarrella, M. C. (2021). Ionic tactile sensors as promising biomaterials for artificial skin: Review of latest advances and future perspectives. *European Polymer Journal*, 151, 110421. <https://doi.org/10.1016/j.eurpolymj.2021.110421>
- [13] Saini, L., Kumar, A., Naaz, A., Ali, A., Saxena, P. & Singh, V. (2023). Herbal Hair Serum: Design, Development & Evaluation. *PriMera Scientific Medicine and Public Health*, 3, 18-22. <https://doi.org/10.56831/psmph-03-073>
- [14] Heo, S., Kim, C., Kim, T. & Park, H. (2020). Human-Palm-Inspired Artificial Skin Material Enhances Operational Functionality of Hand Manipulation. *Advanced Functional Materials*, 30, 2002360. <https://doi.org/10.1002/adfm.202002360>
- [15] Vijayanchali, S. S. (2017). Nutrient, Phytonutrient and Antioxidant Activity of the Dried Rose Petals. *Journal of Research, Extension and Development*, 6, 36-39. <https://ssrn.com/abstract=3345537>
- [16] Ní Annaidh, A., Bruyère, K., Destrade, M., Gilchrist, M. D. & Otténio, M. (2012). Characterization of the anisotropic mechanical properties of excised human skin. *Journal of the Mechanical Behavior of Biomedical Materials*, 5, 139–148. <https://doi.org/10.1016/j.jmbbm.2011.08.016>
- [17] Nazali, N. N. M., Anirad, N. A. A. & Manan, N. F. A. (2020). The Mechanical Properties of Mimic Skin, *Applied Mechanics and Materials*, 899, 73–80. <https://doi.org/10.4028/www.scientific.net/amm.899.73>
- [18] Groves, R. B., Coulman, S. A., Birchall, J. C. & Evans, S. L. (2013). An anisotropic, hyperelastic model for skin: Experimental measurements, finite element modelling and identification of parameters for human and murine skin. *Journal of the Mechanical Behavior of Biomedical Materials*, 18, 167–180. <https://doi.org/10.1016/j.jmbbm.2012.10.021>
- [19] Mihai, L. A., Woolley, T. E. & Goriely A. (2019). Likely equilibria of the stochastic Rivlin cube. *Philosophical Transactions of the Royal Society A: Mathematical, Physical and Engineering Sciences*, 377, 20180068. <https://doi.org/10.1098/rsta.2018.0068>
- [20] Manan, N. F. A., Mahmud, J. & Ismail, M. H. (2013). Quantifying the Biomechanical Properties of Bovine Skin under Uniaxial Tension, *Journal of Medical and Bioengineering*, 2, 45–48. <https://doi.org/10.12720/jomb.2.1.45-48>